Interaction of Hydrogen Chloride with Thin Ice Films: The Effect of Ice Morphology and Evidence for Unique Surface Species on Crystalline Vapor-Deposited Ice

V. Sadtchenko,† C. F. Giese, and W. Ronald Gentry*

Department of Chemistry, University of Minnesota, Minneapolis, Minnesota

Received: October 25, 1999; In Final Form: July 18, 2000

Temperature programmed desorption mass spectrometry (TPDMS) has been employed to study the interactions of hydrogen chloride with thin (200−1000 ML) ice films prepared under a variety of conditions. A single desorption state, designated as β-HCl, is observed in experiments with ice films vapor-deposited at substrate temperatures below 153 K and in experiments with ice films prepared by annealing of amorphous ice at 170−180 K. β-HCl evolution occurs at 205 K and is consistent with desorption of HCl hexahydrate, $HCl\cdot(H_2O)_6$, incorporated into the ice film bulk. HCl uptake measurements demonstrate that migration of hydrogen chloride into the film bulk is relatively unrestrained even at 100 K. Dramatic differences in HCl TPD spectra and uptake are observed when ice films are vapor-deposited at temperatures above 153 K. A new state, designated as δ-HCl, appears in the TPD spectra at 185 K. HCl uptake with this type of film is limited to approximately 1 ML. δ-HCl is tentatively assigned to desorption of a unique surface bound HCl phase formed exclusively on crystalline ice with a low density of surface defects. The morphologies of annealed and vapor-deposited films and their effects on interactions of hydrogen chloride with ice are discussed.

Introduction

It is now generally accepted that heterogeneous reactions on stratospheric ice particles in the Antarctic region play an important role in ozone loss chemistry.[1,2] The principal constituent of type II polar stratospheric clouds (PSC's) are solid water particles formed at temperatures above 180 K.[1] The environmental importance of the ozone loss problem has stimulated intense laboratory studies of stratospherically relevant heterogeneous reactions. An experimental approach that includes studies of elementary reaction steps on thin (typically <300 ML) H_2O ice films is often adopted.[3−11] Offering the advantages of using standard surface science techniques, this approach, however, has some limitations. The ultrahigh vacuum required for some experiments does not allow for ice film growth under conditions similar to those encountered in the stratosphere.

Depending on pressure and temperature, water ice can exist in a number of structurally different phases. At low pressures (<0.2 kbar), there are three structurally distinct forms of ice: an amorphous phase (Ia), crystalline cubic form (Ic), and crystalline hexagonal phase (Ih). Many experiments have been performed in order to determine temperature ranges for formation of particular forms of ice.[12,13] The results of these experiments vary greatly depending on preparation techniques. With some measure of confidence the temperature ranges for formation of three different forms of ice can be deduced from an overlap in the results from these various experiments.

When grown in a vacuum by vapor deposition on a cold substrate, amorphous ice dominates at temperatures below 130 K. Low-density amorphous ice (r < 0.93 g/cm^3) is usually microporous.[14−16] From 130 to 155 K a mixture of amorphous and cubic ice may exist.[13] At temperatures above 160 K ice is expected to be fully crystalline, though cubic and hexagonal forms may coexist. At temperatures above 180 K, vapor deposition on a cold substrate is likely to result in crystalline hexagonal ice.[12]

Crystalline ice can be prepared also by annealing of amorphous ice at temperatures above 160 K.[13] The ice films in high vacuum experiments are usually conducted with amorphous ice films or with crystalline ice films prepared by annealing of the amorphous ice samples at 150−170 K. It has been a matter of concern that the structures and reactivities of such ice films may differ significantly from those of stratospheric ice particles.[15,16] The porosity of amorphous films depends dramatically on the temperature and rate of H_2O deposition. Zondlo et al. have demonstrated that the H_2O partial pressure required for deposition of relatively pore-free ice films must be below 10^{-9} Torr at 95 K.[15] The annealing of such microporous amorphous ice may produce crystalline ice samples which have microstructures different from those of ice films prepared by vapor deposition at temperatures above 150−160 K.

Morphology may have a significant effect on the reactivity of ice films. Adsorption, desorption, surface mobility, and bulk diffusion of reagents and reaction products may all depend dramatically on the ice microstructure. Pores have been observed to facilitate trapping of large quantities of gases in the bulk of amorphous ice films.[14,17] A high density of surface defects may also lead to an increase in the hydrogen bonding abilities of crystalline ice. Disparities in the results from experiments with thin amorphous and crystalline annealed films indicate that the importance of ice film morphology is often underestimated. For example, Hanson and Ravishankara observed that HCl uptake at the surface of ice prepared by vapor-deposition at temperature above 180 K was limited to about a monolayer.[19] George et al. obtained similar results with ice films prepared by vapor deposition at temperatures above 160 K.[20] Roberts et al., however, reported almost unrestricted migration of HCl into the ice bulk in experiments with thin amorphous and crystalline annealed films.[10]

* Corresponding author.
† Present address: Department of Chemistry, Indiana University, Bloomington, IN.

10.1021/jp9937860 CCC: $19.00
Published on Web 09/16/2000

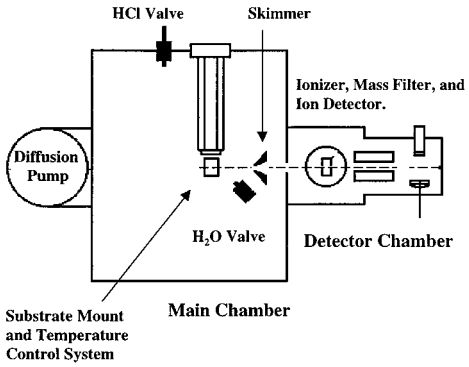

Figure 1. Schematic representation of the experimental apparatus showing the principal features. Features are not shown to scale.

Using temperature programmed desorption mass spectrometry (TPDMS) we have investigated the interaction of hydrogen chloride with ice films prepared under a variety of conditions. The differences in the reaction pathways of HCl adsorbed on three types of ice films, (1) microporous amorphous (MA), (2) crystalline annealed (CA), and (3) crystalline vapor-deposited (CD), are the focus of this work. Using HCl as a molecular probe we have attempted to infer the morphologies of different types of ice. In the following sections we provide experimental evidence that HCl/H_2O interactions at the surface of crystalline vapor-deposited ice are dramatically different from those of amorphous and crystalline annealed ice.

Experimental Section

A schematic diagram of the apparatus is shown in Figure 1. The instrument modified for this work was previously used for crossed beam measurements of differential cross-sections for inelastic and reactive scattering and photodissociation experiments.[21] The experiments were conducted in a vacuum chamber pumped with a Varian HS-20 oil diffusion pump. During TPDMS experiments the main chamber was maintained at background pressures $<5 \times 10^{-7}$ Torr. H_2O vapor was admitted into the chamber using a direct doser consisting of a stainless steel tube terminated in a solenoid valve. H_2O ice films were vapor-deposited on a platinum substrate 5 mm in diameter and 0.5 mm thick. The substrate was in thermal contact with a liquid nitrogen cooled reservoir. A tungsten filament was positioned behind the substrate. Between 95 and 800 K, the substrate temperature was varied through a balance of radiative heating from the filament and thermal conductance to the cold reservoir. Heating/cooling rates in excess of 100 K/s were achieved with this experimental arrangement. The temperature was monitored with a copper−constantan thermocouple junction spot-welded to the edge of the substrate.

The substrate was positioned on the line of sight of a quadrupole mass spectrometer detector. The mass spectrometer employed a custom built electron impact ionizer and a Daly type ion detector. The detector chamber consisted of two differentially pumped regions. The outer region, which contained the quadrupole mass filter, ion optics, and the ion detector, was maintained at $\sim 5 \times 10^{-9}$ Torr. The inner region, which contained the electron impact ionizer, was maintained at 5×10^{-10} Torr. A skimmer placed between the substrate and the detector allowed only desorption products generated at the substrate to enter the detector and blocked any direct path to the detector from parts of the substrate mount which may experience heating during TPDMS experiments.

A typical TPDMS experimental cycle began with cleaning of the substrate. Volatiles were removed from the substrate surface by heating of the substrate to 500K for 20−50 s. The substrate was then rapidly cooled to the desired temperature, and an ice film was deposited. When required, the ice film could be annealed after deposition. In experiments with HCl, the ice films were dosed with hydrogen chloride by pressurizing the main chamber with pure gaseous HCl or with a HCl/helium mixture. In all experiments, the HCl partial pressure, as monitored with an ion gauge, was maintained at $\sim 5 \times 10^{-6}$ Torr during deposition. After the ice film preparation and HCl dosing, a TPDMS spectrum was obtained. This experimental cycle was repeated as desired, with varying annealing conditions, HCl deposition conditions, and H_2O deposition conditions. All steps in the experimental cycle were fully automated via computer.

The vacuum conditions in our experiments raise concerns about ice surface contamination. We have determined, however, that the background gas condensation rate at the ice surface was less than 0.005 ML/s. The main "contaminant" was background H_2O. The time scales of our TPDMS experiments were short in comparison with the evaporation lifetimes of the ice films.

The advantages of our approach are numerous. First, due to a very high pumping speed, we were able to conduct direct rate measurements of desorption kinetics. Careful testing demonstrated that, in desorption experiments, signals due to direct desorption from the substrate surfaces were at least 2 orders of magnitude higher than signals due to the increase of the partial pressures of desorption products in the main chamber. Second, we were able to employ TPDMS in experiments with relatively thick (200−2000 ML) H_2O ice films. It has been demonstrated that interactions with the substrate can affect the microstructure and crystallization kinetics of ice films. The substrate influence, however, was observed to be significant only for ice films which were less than 50 monolayers thick.[22] The influence of the underlying platinum substrate on the morphology and reactivity of the ice surface was therefore minimal in our experiments. Finally, our approach allowed for very high water deposition rates without fatal increases in background pressure. As a result we were able to grow ice films under conditions close to those encountered in the stratosphere.

Results and Discussion

Isothermal Desorption. Isothermal desorption studies were conducted in order to characterize the morphologies of CA and CD ice. Approximately 2000 ML thick CD ice films were prepared by H_2O-vapor deposition at 173 K. The H_2O flux during the ice film growth was ~ 20 ML s^{-1}. The procedures for estimation of the H_2O flux and the ice film thickness are described in the Appendix. After deposition the ice films were cooled to 95 K.

CA ice films were prepared by the following procedure. Amorphous ice films, 2000−5000 ML thick, were grown at 95 K by exposing the substrate to a 20 ML s^{-1} flux of H_2O. The amorphous ice films were then annealed for 50−300 s at 173 K. The time of H_2O deposition and time of annealing were chosen to make the thickness of the CA films approximately equal to the thickness of the CD ice films. After annealing, the ice films were cooled to 95 K.

Isothermal desorption (ID) spectra of $\sim$2000 ML thick amorphous, CA, and CD ice films are shown in Figure 2. All spectra were obtained at 170 K following a temperature jump from 95 K. The heating rate during the temperature jump was approximately 100 K/s. The CA and CD ice films clearly demonstrate zero-order sublimation kinetics. In the case of

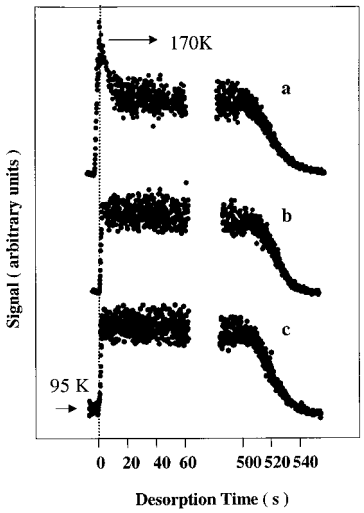

Figure 2. Isothermal desorption spectra of ∼2000 ML thick amorphous (a), crystalline annealed (b), and crystalline vapor-deposited (c) ice films.

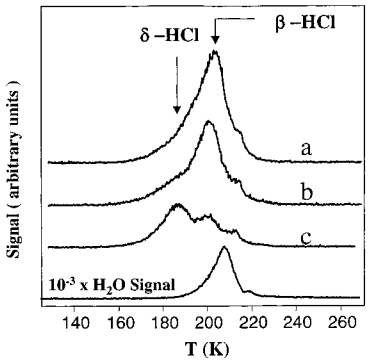

Figure 3. TPD spectra of HCl from ∼1000 ML thick amorphous (a), crystalline annealed (b), and crystalline vapor-deposited (c) ice films. HCl exposure was 10^{-4} Torr s. The HCl TPD spectrum from the crystalline ice films, prepared by annealing of an amorphous ice samples (crystalline annealed ice), is similar to HCl TPD from the amorphous ice film. The HCl TPD spectrum from the crystalline ice film vapor-deposited at 173 K is remarkably different from the HCl TPD spectra from both amorphous and annealed ice films.

amorphous ice films, the sublimation rate decreases for the first 25−30 s, then exhibits zero-order kinetics. For all types of ice films, the sublimation kinetics changes when about 98% of the ice film has sublimed.

The ID spectra for the three types of ice are similar to the ID spectra previously reported for sublimation of thin (10−100 ML) amorphous ice films deposited on clean platinum and graphite substrates.[23,24] The high initial sublimation rate of amorphous ice indicates that crystallization is not complete during the temperature jump. The desorption rate decreases as the amorphous ice undergoes crystallization simultaneously with sublimation. The zero-order desorption kinetics consistent with sublimation of a uniform multilayer phase is observed after crystallization is complete. The observed change in sublimation kinetics takes place for all types of ice when the ice films reach a critical thickness of about 20 ML. The breaking of a very thin film into 3D islands or droplets is probably forced by interactions with the substrate at this point.[23,24]

Several important conclusions can be derived from these sublimation kinetics measurements. First, crystalline ice samples prepared by annealing of amorphous ice films, as well as crystalline ice samples prepared by vapor deposition at 173 K, are smooth, solid, and free of large pores. The sublimation kinetics should be sensitive to the structure of the films, i.e., any kind of ice surface roughening or smoothing during sublimation should lead to changes in the effective surface area of the film and, thus, to changes in the sublimation rate.

Second, CD as well as CA ice films are fully crystallized and have similar phase compositions. Isothermal desorption spectra of amorphous ice demonstrate that incomplete crystallization should manifest itself in non-zero-order sublimation kinetics. Significant distinctions in the phase composition of crystalline ice films should result in different sublimation rates. The sublimation rates of CA ice films, however, are very close to the sublimation rates of CD ice films. It should be pointed out, however, that we have no experimental means to determine precisely the crystalline structure of our crystalline ice films. It is unclear whether CD and CA ice films are composed of cubic, hexagonal, or a mixture of both types of crystalline ice.

Third, since the amorphous ice films demonstrate zero-order sublimation kinetics after crystallization, these films, though microporous, cover the substrate completely. Indeed, it seems unlikely that if large clusters or islands of amorphous ice were formed instead of relatively uniform film, they would produce a smooth solid crystalline ice film upon crystallization. To confirm this last conclusion, we briefly investigated isothermal desorption and TPD spectra of a multilayer CCl_4 film covered with 1000−2000 ML of amorphous ice. These measurements clearly demonstrate that no CCl_4 evolution into the gas phase occurs until about 90% of the amorphous ice film has desorbed. The results of these experiments are similar to the results obtained by Smith et al. in experiments with thin CCl_4 ice films covered with 50−200 ML of D_2O ice.[25] A dramatic decrease in the sublimation rates of CCl_4 films covered with 1000 ML of amorphous ice demonstrates that ice films of this thickness cover the entire surface of the platinum substrate. Although some of the pores may be interconnected, it is hard to believe that any significant number of gas phase molecules can reach the substrate without undergoing multiple collisions with amorphous ice. Therefore, in the case of HCl reactions with amorphous ice films, most of the gaseous HCl would react within the top layers of the ice films since the sticking probability of HCl on amorphous and crystalline ice is nearly unity at the temperatures present in our experiments.[3,4]

It also follows from these experiments that structural changes during the phase transition from amorphous to crystalline ice do not lead to formation of large ruptures in the bulk of the ice films. The last conclusion does not contradict results obtained by Smith et al.[25] They have observed an abrupt desorption of carbon tetrachloride in TPD experiments with D_2O/CCl_4 films, driven by crystallization of the overlaying amorphous ice. The H_2O ice films in our experiments, however, are significantly thicker compared to the ice films studied by Smith et al. (< 260 ML). We were able to reproduce the results of these researchers in experiments with much thinner H_2O and D_2O (<100 ML) ice films.

Temperature Programmed Desorption. TPD spectra of HCl from MA, CA, and CD ice films are shown in Figure 3. In these experiments, the thickness of the ice films was approximately 1000 ML and the HCl exposure was 10^{-4} Torr s. During HCl deposition, the ice films were maintained at ∼100 K. A TPD spectrum for sublimation of a pure, 1000 ML thick H_2O ice film is shown for reference. In this case the H_2O signal was monitored at *m*/*e* 20 ($H_2{}^{18}O^+$) in order to prevent saturation of the mass spectrometer detector by the intense signal associated with *m*/*e* 18 ($H_2{}^{16}O^+$). The small HCl exposure in these experiments was insufficient to affect noticeably the H_2O TPD

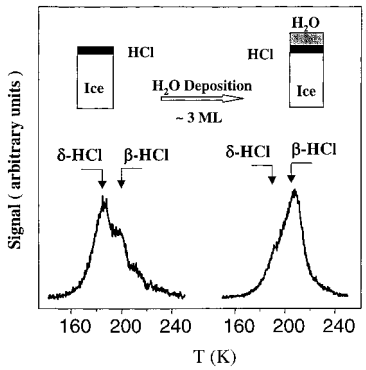

Figure 4. TPD spectra of HCl from a sandwich, amorphous/HCl/crystalline, ice film (right) and from a crystalline vapor-deposited film. The crystalline ice film thickness and HCl exposure are ~1000 ML and 10^{-4} Torr s, respectively. Upon condensation of 2−3 ML of H_2O on the top of the crystalline film exposed to HCl, almost complete conversion of δ-HCl into β-HCl is observed.

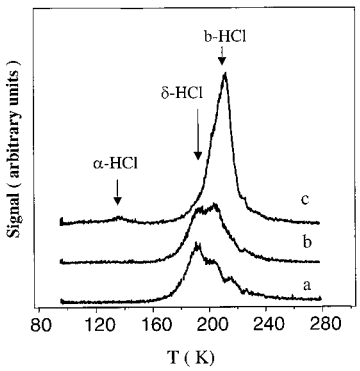

Figure 5. TPD spectra of HCl from ~1000 ML thick crystalline vapor-deposited films at different HCl exposures. HCl exposures are 10^{-4} Torr s (a), 3×10^{-4} Torr s (b), and 10^{-3} Torr s (c). δ-HCl slowly converts into β-HCl with increasing exposure. A new feature, α-HCl, appears in the TPD spectra at high HCl exposures.

spectra at this detector sensitivity; i.e., no temperature shift or narrowing was observed for the H_2O sublimation peak. The H_2O TPD spectra of 1000 ML thick amorphous, CA, and CD ice films were essentially identical at this detector sensitivity.

The TPD spectra of HCl from MA and CA ice films are similar and consist of a single asymmetric peak, designated as β-HCl.[10] A small shoulder at ~ 220 K is shifted by about 8 K toward higher temperatures with respect to the H_2O sublimation peak maximum. This TPD feature probably represents the residual HCl/H_2O interaction with the underlying substrate and will not be discussed further.

In the case of the TPD spectrum of HCl from CA, as well as from MA, there is a significant overlap between the HCl and H_2O TPD spectra; the maximum rate for HCl evolution into the gas phase is achieved when ~30% of the H_2O has already desorbed. The concurrent evolution of H_2O and HCl into the gas phase indicates that these TPD spectra correspond largely to desorption of hydrogen chloride which has been incorporated into the ice film bulk.

HCl hexahydrate, $HCl(H_2O)_6$, has been shown previously to form as a result of limited exposure of amorphous and CA ice films to gaseous HCl under similar experimental conditions.[6−10] HCl hexahydrate may be formed either directly upon exposure of the ice films to gaseous HCl at 100 K or as the product of a thermally enabled reaction during TPD. We conclude from our measurements that the final products of HCl/H_2O reactions at the surfaces of CA and amorphous microporous ice are essentially identical and consistent with formation of the HCl hexahydrate previously observed by others.

A dramatically different TPD spectrum of HCl, however, is observed in the case of desorption from CD ice films. First, HCl adsorption on CD ice films results in significantly lower β-HCl yield. Second, a new TPD feature, designated as δ-HCl, appears at 185 K. Comparison of the HCl and H_2O TPD spectra reveals that δ-HCl evolution occurs before a significant part of the H_2O film has desorbed. This indicates that, unlike β-HCl, δ-HCl is derived from hydrogen chloride confined to the surface of the CD film.

A simple experiment that further supports this conclusion was conducted. An equivalent of ~3 ML of H_2O was condensed on the surface of a CD ice film after the ice film had been exposed to 10^{-4} Torr s of gaseous HCl. The TPD spectrum of HCl from the resulting sandwich H_2O/HCl/ice film is displayed in Figure 4, which shows nearly total conversion of δ-HCl into β-HCl. A significant decrease in the δ-HCl yield upon deposition of an amorphous ice adlayer clearly demonstrates that the δ-HCl peak originates from hydrogen chloride located on the surface and not in the bulk of the CD ice film.

A β-HCl peak, consistent with the desorption of HCl hexahydrate, is present along with the δ-HCl peak in the TPD spectra for HCl evolution from CD ice films. It is tempting to assign the δ-HCl peak to the desorption of an HCl/H_2O adlayer formed exclusively at the surface of HCl hexahydrate. We have observed, however, that while the total HCl uptake by CD ice films remains nearly the same, δ-HCl appears to convert into β-HCl with increasing HCl exposures. The TPD spectra of HCl for several HCl exposures are shown in Figure 5. Conversion of δ-HCl into β-HCl at high HCl exposures is inconsistent with formation of an HCl adlayer at the surface of the HCl hexahydrate, since an increase in the β-HCl yield should be accompanied in this case by a proportional increase in the δ-HCl yield. Furthermore, careful examination of the HCl TPD spectra in case of a large (~10^{-3} Torr s) HCl exposure reveals a weak peak at ~145 K. This peak is consistent with α-HCl, a feature which has been observed in TPD spectra of HCl from thin amorphous and CA films saturated with hydrogen chloride.[6,10] α-HCl was attributed either to desorption of molecular HCl adsorbed at the surface of HCl hexahydrate[10] or to the decomposition of a thin HCl monohydrate adlayer formed on saturated hexahydrate films.[6] Once destroyed by brief annealing above 140 K, the α-HCl TPD feature was observed to recover after repeated exposure of the hexahydrate films to HCl. The conversion of δ-HCl into β-HCl, however, appears to be irreversible. Any attempt to redeposit δ-HCl after the conversion has been accomplished leads only to formation of a very weak feature at 145 K. *These observations support the conclusion that the* δ-HCl *peak is associated with a unique adsorbed state of HCl which is characteristic of the surface of crystalline vapor-deposited ice and is essentially absent at the surface of crystalline annealed and amorphous ice.*

To our knowledge, δ-HCl has never been observed before in TPDMS experiments with thin ice films. We speculate that δ-HCl is associated with desorption of a unique surface bound HCl phase, formed solely at the surface of CD films. The existence of such a surface bound HCl phase has been recently suggested by Devlin et al.[29] An example of such a state would be a lower hydrate $HCl(H_2O)_{n(\text{surface})}$ ($n = 1-3$) formed solely at the ice surface. We should emphasize that such a hydrate formed on the surface of crystalline ice may differ significantly from lower HCl hydrates, formation of which was previously observed as a result of saturation of ice bulk with HCl at high partial pressures.[20,26−28] Assuming that HCl hexahydrate is the most thermodynamically stable species at the temperatures and

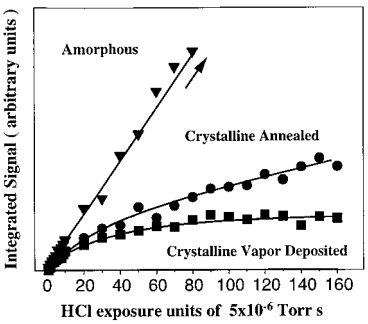

Figure 6. HCl uptake, derived from TPD spectra, at the surface of amorphous ice (triangles), crystalline annealed (circles), and crystalline vapor-deposited (squares) ice films. Unlike amorphous and annealed ice films, the crystalline ice, prepared by H_2O vapor-deposition at 173 K, displays saturation of the HCl uptake.

pressures present in our experiments, our assignment of the δ-HCl peak to desorption of surface bound HCl phase is consistent with the observed irreversible conversion of δ-HCl into β-HCl.

Validation of studies of the exact nature of surface bound HCl phase is a matter for future research; however, the significance of our comparative TPD measurements is apparent. Comparison of the TPD spectra for HCl evolution from different types of ice unambiguously demonstrates that the HCl/H_2O reaction pathways at the surface of CD ice can be quite different from the HCl/H_2O reaction pathways on CA and MA ice.

HCl Uptake. The HCl yields for various HCl exposures were determined from time-integrated TPD spectra, with the results shown in Figure 6. Exposure of MA ice to gaseous HCl results in the highest HCl yields from the film. High HCl yield in the case of amorphous ice is expected, since under our H_2O deposition conditions (high H_2O flux, low deposition temperature) the resulting amorphous ice films should be highly porous. The high microscopic porosity of this type of ice results in a large effective surface area of the films, providing a very large number of adsorption sites for HCl. The HCl yield from this type of ice grows rapidly with HCl exposure. The linear dependence of HCl yield on the HCl exposure probably indicates rapid migration of HCl into the amorphous ice bulk, since the surface adsorption sites are not being saturated in the experimental exposure range.

In the case of CA ice films, the HCl yield grows rapidly at HCl exposures below 5×10^{-5} Torr s, slowing by about a factor of 2 at higher HCl exposures. The HCl yield from CA ice, similar to the HCl yield from MA ice, does not saturate over the entire range of HCl exposures studied. The gradual increase in HCl yield at high exposures is consistent with slow migration of HCl into the bulk of the CA ice films. These measurements are consistent with previously reported results from TPD experiments on HCl interactions with nanoscale amorphous and crystalline annealed ice films.[6,10] HCl yields from amorphous and crystalline annealed ice films were observed to increase until the entire bulk of the ice film was saturated with HCl.

The situation is different in the case of CD ice films. The HCl yield grows rapidly at HCl exposures below 5×10^{-5} Torr s. However, at an HCl exposure of approximately 3×10^{-4} Torr s, the HCl yield from CD ice films reaches a plateau, indicating that no further hydrogen chloride adsorption occurs at greater exposures. The limited HCl yield in the case of CD ice cannot be explained by saturation of the entire ice film bulk with HCl. The maximum HCl yield was essentially independent of the ice film thickness. For coverages between 200 and 2000 ML, the maximum HCl yield increased by less than 3%. The saturation of the HCl yield at exposures above 3×10^{-4} Torr s implies that the HCl uptake is limited by the ice film surface area. Comparison of the integrated TPD signals for HCl and H_2O allows us to estimate the absolute HCl uptake. Assuming that the cross-section for HCl ionization in the electron-bombardment ionizer of the mass spectrometer is about half that for H_2O,[10] the upper limit for the maximum HCl yield from the CD ice was determined to be 1 ML ($\sim 10^{15}$ cm^{-2}).

These measurements clearly demonstrate that HCl uptake at the surface of crystalline ice films depends on the conditions under which the films are prepared. The observed rate of HCl migration into the bulk of the CD ice films is extremely low at 100 K. The HCl uptake by the CD ice films is limited to about 1 ML. In contrast, the HCl uptake by CA ice is not confined to the surface area of the ice film. Similar to microporous amorphous ice, HCl migration into the bulk of CA ice films is apparent even at 100 K.

Model of HCl Interactions with Polycrystalline Ice Film. It should be noted that both CD and CA ice films are expected to be polycrystalline. HCl/H_2O reaction pathways for HCl adsorbed on grain boundaries may differ significantly from those of HCl adsorbed on the surfaces of crystallites. Indeed, the formation of HCl hexahydrate at the surface of ice crystallites must require extensive adsorbate-induced lattice reconstruction, leading to high barriers for hydration. The grain boundaries and other surface defects, characterized by a high degree of disorder in the hydrogen bond network, may, however, provide unique HCl adsorption sites with significantly lower barriers for formation of higher HCl hydrates.[30,31] Considering these facts, it is easy to rationalize the results of TPD experiments with CD and CA ice. Only three essential assumptions are necessary:

1. The adsorption of HCl on the surfaces of crystallites leads to formation of a unique surface bound HCl phase, which is different from HCl hexahydrate. However, adsorption of HCl on the grain boundaries facilitates formation of HCl hexahydrate.

2. The diffusion of molecular HCl through the adlayer of surface bound HCl is very slow at 100 K. Indeed, as shown in Figure 5, the HCl TPD spectrum from CD ice changes with increasing HCl exposure. At HCl exposure of 10^{-4} Torr s, the HCl TPD spectrum is consistent with desorption of surface bound HCl. As the HCl exposure increases, the spectra change and become similar to the desorption spectra of HCl hexahydrate. The HCl yield, however, does not change significantly at HCl exposures above 10^{-4} Torr s and is equal to approximately 1 ML.

3. Unlike diffusion of HCl through an adlayer of HCl phase formed on the surfaces of crystallites, the diffusion of molecular HCl through HCl hexahydrate, formed along the grain boundaries, is relatively rapid even at 100 K. This assumption can be easily justified. Indeed, the formation of HCl hydrate along the grain boundaries may lead to a significant decrease in the intermolecular distances between some H_2O molecules. As a result, pores or ruptures may form at the interfaces between crystallites. Thus, HCl hexahydrate formed along grain boundaries may become a conduit for migration of molecular HCl in the bulk of the polycrystalline ice films.

The details of this model of HCl interactions with polycrystalline ice is illustrated in Figure 7. As shown in Figure 7a, upon adsorption at 100 K, hydrogen chloride may react with ice to form a surface bound HCl state at the surfaces of crystallites and HCl hexahydrate at the grain boundaries. If the HCl phase, formed on the surfaces of crystallites, is impermeable to gaseous HCl at 100 K, the amount of hydrogen chloride adsorbed in this form would quickly saturate and would be

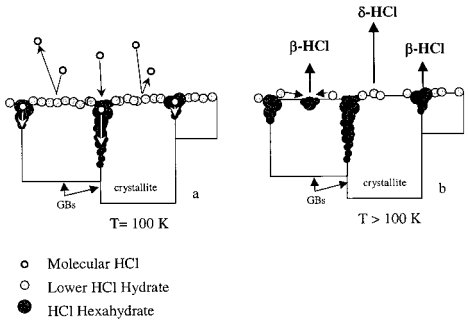

Figure 7. Model of HCl reaction pathways on polycrystalline ice.

limited to less than one monolayer. The opposite is true for uptake of HCl on grain boundaries. If the diffusion of HCl through HCl hexahydrate formed along the grain boundaries is possible, HCl uptake in the form of HCl hexahydrate is likely to increase with exposure until the entire grain boundary network is saturated with HCl hexahydrate. The rate of HCl uptake in the form of HCl hexahydrate, however, must depend on the average size of the crystallites. Thus, if the average grain diameter is large, i.e., the grain boundaries are rare, the amount of HCl hexahydrate formed at a particular exposure is relatively small.

As shown in Figure 7b, during TPD the surface bound HCl may either desorb or react to form HCl hexahydrate. Thus, the desorption of surface bound HCl at 185 K gives rise to the δ-HCl peak, and the desorption of HCl hexahydrate results in the β-HCl peak in the TPD spectra. For a particular polycrystalline ice film, the δ- and β-HCl yields must depend strongly on the grain size distribution. On ice films with a large average grain diameter, first, the adsorption of HCl in the surface bound form should dominate, second, the total HCl uptake must be low, and third, the HCl migration into the ice film bulk along the grain boundaries should be slow. As a result, the TPD spectra of HCl from ice films with relatively large average grain size should be characterized by a pronounced δ-HCl peak and a low total HCl yield.

TPD experiments with CD ice films of variable thickness strongly support our model of HCl/ice interactions. To verify the proposed mechanism of HCl interactions with polycrystalline ice films, we attempted to modify the grain-size distributions of these films. The approach we used is based on the fact that in thin films of polycrystalline material the average grain size under conditions of uninhibited grain growth is about twice the film thickness (thin film limit).[32] If indeed such conditions are present during vapor-deposition of ice films at 173 K, the average grain size in CD ice should increase proportionally with the ice film thickness. Therefore, if our model of HCl interactions is correct, the increase in CD ice film thickness must result in higher δ-HCl yield as shown in Figure 8a. TPD spectra of HCl from 200, 1000, and 2000 ML thick polycrystalline vapor-deposited ice films are shown in Figure 8b. In all cases the ice films were vapor-deposited at 173 K, and the HCl exposure was 10^{-4} Torr s at 100 K. As predicted, an increase in the film thickness results in higher δ-HCl yields and significantly lower β-HCl yields. These results unambiguously demonstrate that, in agreement with our simple hypothesis and the theoretical predictions of others,[30,31] the abundance of grain boundaries and related surface defects has a profound effect on the HCl/ice reaction pathways.

In the case of CA ice, the β-HCl peak associated with the desorption of HCl hexahydrate dominates the TPD spectra. Furthermore, compared to the HCl yield from CD ice, the HCl yield from CA increases much more rapidly with HCl exposure, indicating that rapid HCl migration into the bulk occurs rapidly

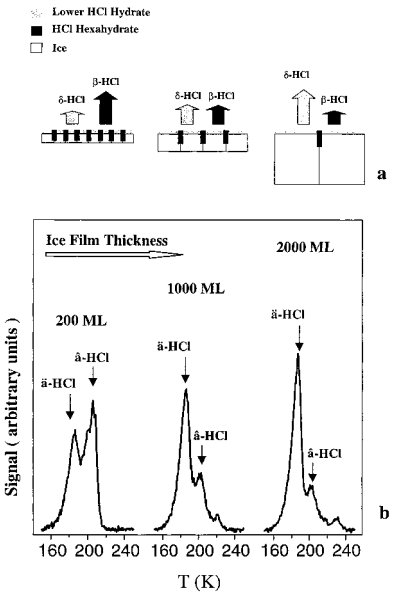

Figure 8. TPD spectra of HCl from crystalline vapor-deposited films of different thicknesses. HCl exposure is 10^{-4} Torr s. The δ-HCl yield is higher and the β-HCl yield is lower for thicker ice films.

even at 100 K. *Therefore, we conclude that the microstructures of the CA and CD ice films differ significantly in their grain-size distributions, with polycrystalline annealed ice films having a much smaller average grain size, and therefore a much higher density of grain boundaries.*

Our hypothesis provides a ready explanation for the apparent lack of significant distinctions in isothermal desorption spectra of pure CD and CA ice. Unlike pores or ruptures, the interfaces between crystallites do not necessarily increase the effective surface area of the films. Grain boundaries in the bulk of an ice film, thus, are not expected to enhance the ice sublimation rate by simply raising the effective surface area of the film. In comparison with H_2O desorption from the faces of grains, the desorption of H_2O from grain boundaries should be characterized by a different rate. The ratio of the net surface area of the grain boundaries to the net open surface area of the crystallites, however, may be quite low and should be roughly inversely proportional to the grain diameter. Therefore, even at relatively small average grain size, the contribution of H_2O desorption from the grain boundaries to the overall sublimation kinetics may be too small to detect.

Alternative Hypothesis. An alternative hypothesis for the observed differences in interactions of HCl with CD and CA ice needs to be discussed. One can argue that our experimental results can be explained without taking into consideration the grain size distribution in CD and CA ice films. Indeed, the surface morphology of CD and CA ice can be different in terms other than average crystallite size. For example, in the case of CA ice, prolonged annealing of amorphous ice films may lead first to crystallization and then to relaxation of the crystalline ice surface. As a result, the interfaces of crystallites will be disordered and the number of dangling hydrogen bonds will be minimized.[33,34] In the case of CD ice such surface relaxation may not be possible since we usually cooled our CD ice films to 95 K shortly after CD ice film deposition was completed. Crusts of different HCl hydrates may form on the surfaces of CA and CD ice as a result of such distinctions in their surface morphology. The differences in the HCl uptake on CD and CA ice, thus, can be explained merely by different rates of diffusion through two types of HCl hydrate crusts.

This alternative hypothesis, though simple, has several apparent shortcomings. For example, it fails to provide an explanation for the observed dependence of the HCl TPD spectra on CD ice film thickness. Indeed, the structure of the top layers of CD ice must depend on the conditions present at the moment of termination of the deposition sequence. If one disregards the differences in the grain size distribution, one should expect the surfaces of the CD ice films of various thicknesses to be identical, since the temperature and H_2O flux do not vary during ice film growth. As a result the TPD spectra of HCl from CD ice films of various thicknesses should also be identical. However, in the case of CD ice, we have observed a strong dependence of δ- and β-HCl yields on the ice film thickness. Furthermore, experiments with CD ice films, which were also annealed at 170 K prior to HCl deposition, demonstrated that HCl TPD spectra from such annealed CD ice films were identical to the TPD spectra from regular CD ice films.

In the case of CA ice films, the δ-HCl peak is completely absent from the TPD spectra. One thus can argue that this result is inconsistent with the proposed hypothesis since, even if the average grain size is relatively small, the surface of polycrystalline ice cannot consist solely of grain boundaries. A small δ-HCl feature should therefore be present in the TPD spectra. We would like to emphasize that the δ-HCl and β-HCl yields cannot be directly used in order to infer the relative abundances of HCl adsorption sites at the surfaces of crystallites and at the grain boundaries. Indeed, the observed conversion of δ-HCl into β-HCl at 100 K indicates that a surface bound HCl on the crystallites can still react slowly to form HCl hexahydrate. Thus, as shown in Figure 7b, the δ-HCl yield is the result of the competition between the desorption of the surface bound HCl and conversion of this HCl phase into HCl hexahydrate during TPD. The fact that the δ-HCl peak is observed in the TPD spectra of HCl on the CD ice films indicates that a significantly larger amount of surface bound HCl is initially present on this type of ice films.

Grain Growth in CA Ice. It is important to understand the mechanism that leads to the formation of extremely fine grain structures in polycrystalline films prepared by annealing of amorphous ice. The distribution of matter in the bulk of a thin film prepared under conditions of ballistic deposition is characterized by significant microscopic density fluctuations.[35] In the case of amorphous H_2O ice films, the local density maxima are likely to become nucleation centers during the annealing of the film.

The normal grain growth can be drastically inhibited if pores are present in the bulk of the film undergoing crystallization.[36] The pores, similar to precipitates, inhibit grain boundary motion. Fine-grained oxide ceramics, for example, are prepared by sintering of powdered ceramics.[37] In a crystallizing porous ice film, microscopic voids are likely to be arranged along grain boundaries. This may lead to significant constraint of the grain growth, such that the mean grain size never reaches the thin film limit. Polycrystalline annealed ice films, therefore, may consist of grains with an average size on the order of the size of density fluctuations in the bulk of the amorphous ice. The spatial separation between local density maxima under ballistic deposition conditions is determined by deposition flux fluctuations and may be only a few molecular diameters on average.[27]

We have also investigated the effect of prolonged annealing on the HCl TPD spectra. An increase in the annealing time from the usual 50 s to about 300 s at 173 K produced essentially no effect on the TPD spectra of HCl. Apparently, longer annealing does not significantly affect the microstructure of the films. This demonstrates that at 173 K the grain growth is inhibited. To promote grain growth, annealing should be carried out at higher temperatures. However, considering that the sublimation rate at 173 K is already relatively high, it seems unlikely that large grain polycrystalline ice films can be easily prepared by annealing of amorphous microporous ice samples. Recently, Kay et al. utilized a well-collimated molecular beam in order to deposit amorphous ice films. Their measurements demonstrated that vapor deposited amorphous ice films can be virtually free of micropores if the H_2O beam is directed normal to the substrate.[38] Perhaps annealing of such pore-free amorphous ice samples may produce crystalline ice with a relatively large grain size.

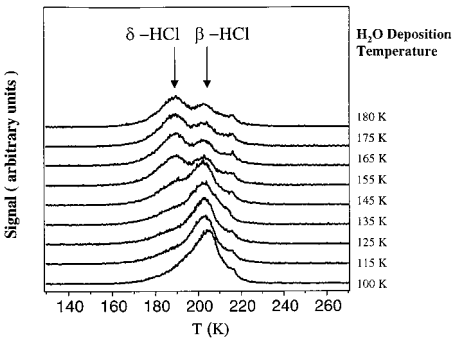

Figure 9. TPD spectra of HCl evolution from ∼1000 ML thick ice films vapor-deposited at different temperatures. The HCl exposure was 10^{-4} Torr s.

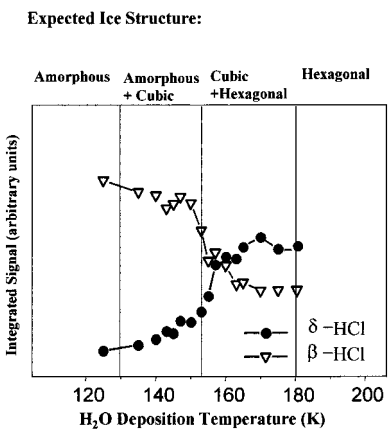

Figure 10. δ-HCl and β-HCl yields from ice films vapor-deposited at different temperatures. The HCl exposures and film thicknesses are 10^{-4} Torr s and ∼1000 ML, respectively.

Dependence of the HCl TPD Spectra on Ice Deposition Temperature. To determine the appropriate experimental conditions for crystalline ice film preparation and to further demonstrate the effect of the film microstructure on HCl/ice reactions, we have measured TPD spectra for HCl evolution from ice films grown at various temperatures. In all experiments, the HCl exposure was $\sim 10^{-4}$ Torr s. The H_2O deposition temperature was varied from 100 to 180 K. The film thickness was kept constant at ∼1000 ML. Selected TPD spectra of HCl from the ice films are shown in Figure 9. The TPD spectra of HCl from ice films vapor-deposited at temperatures between 100 and 150 K are similar to the TPD spectra of HCl from polycrystalline annealed ice films; i.e., only the β-HCl peak is present. However, a sudden change occurs at H_2O deposition temperatures greater than 150 K, where the δ-HCl peak appears.

The evolution of the HCl TPD spectra with ice deposition temperature is illustrated in Figure 10, in terms of the relative β-HCl and δ-HCl yields. The HCl TPD spectra were modeled

as linear combinations of β-HCl and δ-HCl peaks. A TPD spectrum of HCl from a 1000 ML thick ice film deposited at 120 K was used as the β-HCl component of the fitting function. A TPD spectrum of HCl from a ~2000 ML thick ice film vapor-deposited at 173 K was used to infer the shape of the δ-HCl peak.

The amorphous ice phase should dominate the ice film composition at temperatures below 130 K.[12,13] The porosity of amorphous ice is expected to decrease at H_2O deposition temperatures near 130 K.[14−16] It is clear, however, that the reduced porosity of amorphous ice near 130 K does not affect significantly the HCl TPD spectra. The HCl/H_2O reaction pathways are similar for amorphous dense and amorphous microporous ice. These results imply that low cohesiveness of the ice bulk and ice surface chemical properties rather than porosity determine the HCl/H_2O reaction pathways.

At higher temperatures (130 K < T < 150 K), where at least partial crystallization is expected, the TPD spectra of HCl are also dominated by the β-HCl peak. The possibility of a mixed amorphous/cubic crystalline phase cannot be ruled out in this temperature range. Coexistence of cubic and amorphous phases could lead to a high density of bulk and surface defects. The dominating reaction pathway therefore may be formation of HCl hexahydrate.

The β-HCl yield decreases rapidly at H_2O deposition temperatures above 153 K. The decrease in β-HCl yield is accompanied by a proportional increase in δ-HCl yield. Disappearance of the amorphous phase is expected at these temperatures.[12,13] A complete crystallization of the ice films and an increased rate of grain growth should result in a lower density of surface and bulk defects. The formation of bulk incorporated HCl hexahydrate is inhibited and hydrogen chloride interactions at the surfaces of large crystallites begin to dominate. The evolution of the HCl TPD spectra continues up to an H_2O deposition temperature of about 165 K. The weak dependence of the β-HCl and δ-HCl yields on H_2O deposition temperature above 165 K suggests that the mean grain size has reached the thin film limit and the density of surface and bulk defects is minimized.

The above results indicate that HCl/H_2O interactions at an ice surface are extremely sensitive to the ice morphology. Crystalline and amorphous ice vapor-deposited at temperatures below 153 K, as well as crystalline annealed ice, have microstructures and chemical properties different from those of crystalline ice films grown at higher temperatures.

Conclusions

This work demonstrates that ice microstructure and reactivity depend dramatically on preparation conditions. In particular, the influence of ice morphology on hydrogen chloride adsorption and desorption is considerable. It is reasonable to infer that other stratospherically important molecules may demonstrate similar sensitivity to the ice microstructure. Caution should therefore be exercised in inferring reaction rates and mechanisms for stratospheric processes from the results of experiments with ice samples prepared under conditions different from those encountered in the stratosphere.

Appendix

Film Thickness and H_2O Deposition Rate Determination. Isothermal measurements of sublimation rates have been used for the estimation of ice film thickness. The zero-order sublimation rate at a temperature T_s can be calculated from the following equation:

$$\text{rate} = \nu_0 \exp\left(\frac{-E_d}{RT_s}\right) \tag{3}$$

where ν_0 is the zero-order desorption preexponetial factor (2.8×10^{30} molecules cm^{-2} s^{-1})[39] and E_d is the desorption activation energy (48.12 kJ mol^{-1}).[40] A single monolayer of a crystalline ice film contains about 10^{15} molecules cm^{-2} of H_2O molecules.[40] Isothermal measurements of the H_2O sublimation rate at known temperatures, therefore, allowed the calibration of our mass spectrometer in absolute units (ML s^{-1}) with respect to H_2O desorption flux. Integrating the H_2O signal over time, either in isothermal desorption experiments or in TPD experiments, we were able to estimate the thickness of the films in monolayer equivalents.

The H_2O flux at the surface of the substrate during ice film deposition was estimated by using the following procedure. The H_2O valve was opened for 5 s and a thin ice film was grown on the substrate at 95 K. The TPD or ID spectrum of this film was then obtained, and the thickness of the film was calculated. Assuming that the sticking probability for water molecules at 95 K is unity, the H_2O flux near the substrate surface can be estimated in monolayer per second units.

The error in the estimation of ice film thickness depends, first of all, on the error in the desorption activation energy, E_d, and preexponential factor, ν_0. Another obvious source of error arises from the temperature measurements. The thermocouple junctions used for temperature measurements in our experiments can contribute about 1 K error in the temperature measurements. These errors, however, have a systematic character and do not affect the relative thickness measurements. More important is the concern that the temperature at the surface of the ice film can differ significantly from the temperature of the substrate. Zero-order sublimation kinetics, observed in isothermal desorption measurements, indicate that the temperature lag between the platinum substrate and the ice surface is less than 2 K. Several simple experiments have been conducted in order to determine the temperature lag. The dependence of TPD spectra on the film thickness for submonolayer amounts of CCl_4 adsorbed on the surface of annealed ice was studied. The ice film thickness was varied from ~ 200 to ~2000 ML. The TPD spectra for CCl_4 adsorbed on thick ice films did not show any significant shifts toward higher temperatures and are identical to the TPD spectra for CCl_4 desorption from very thin (~10 ML) dense amorphous films.[41] From these experiments, the temperature lag between the substrate and ice film surface was found to be less than 2 K for ice films as thick as 2000 ML.

References and Notes

(1) Solomon, S. *Nature* **1990**, *347*, 347.
(2) Solomon, S. *Rev. Geophys.* **1988**, *26*, 131.
(3) Andersson, P. U.; Nagard, M. B.; Pettersson, J. B. C. *J. Phys. Chem.* **2000**, B *104*, 1596.
(4) Isakson, M. J.; Sitz, G. O *J. Phys. Chem.* **1999**; A *103*, 2044.
(5) Schaff, Jason E.; Roberts, Jeffrey T. *Langmuir.* **1998**, *14*, 1478.
(6) Banham, S. F.; Sodeau, J. R. J.; Horn, A. B.; McCoustra, M. R. S.; Chesters, M. A. *J. Vac. Sci. Technol., A* **1996**, *14* (3), 1620.
(7) Graham, J. D.; Roberts, J. T.; Anderson, L. D.; Grassian, V. H. *J. Phys. Chem.* **1996**, *100*, 19551.
(8) Banham, S. F.; Horn, A. B.; Koch, T. G.; Sodeau, J. R. *Faraday Discuss.* **1995**, *100*, 321.
(9) Horn, A B.; Koch, T.; Chesters, M. A.; McCoustra, M. R. S.; Sodeau, J. R. *J. Phys. Chem.* **1994**, *98*, 946.
(10) Graham, J. D.; Roberts, J. T. *J. Phys. Chem.* **1994**, *98*, 8, 5974.
(11) Horn, A. B.; Chester, M. A.; McCoustra, M. R. S.; Sodeau, J. R. J. *Chem. Soc. Faraday Trans.* **1992**, *88* (7), 1077.
(12) Hobbs, P. V. *Ice Physics*; Clarendon Press: Oxford, 1974.
(13) Eizenberg, D.; Kauzmann, W. *The structure and Properties of water*; Oxford University Press: New York, 1969.

(14) Sadtchenko, V.; Knutsen, K.; Giese, C. F.; Gentry W. R. *J. Phys. Chem.* **2000**, B *104*, 2511.
(15) Zondlo, M. A.; Onasch, T. B.; Warshawsky, M. S.; Tolbert M. A.; Mallick G.; Arentz P.; Robinson M. S. *J. Phys. Chem.* **1997**, *101*, 10887.
(16) Berland, B. S.; Brown, D. E.; Tolbert, M. A.; George, S. M. *Geophys. Res. Lett.* **1995**, *22*, 3493.
(17) Bar-Nun, A.; Owen, T. *Astrophysics Space Sci.-Libr.* **1998**, *227*, 353.
(18) Schaff, J. E.; Roberts, J. T. *J. Phys. Chem.* **1996**, *100*, 14151.
(19) Hanson, D. R.; Ravishankara, A. R. *J. Phys. Chem.* **1992**, *96*, 2682.
(20) Foster, K. L.; Tolbert, M. A.; George, S. M. *J. Phys. Chem.* **1997**, A *101* (27), 4979.
(21) Gentry, W. R. In *Atomic and Molecular Beam Methods*; Oxford: New York, 1988; Vol. 1.
(22) Engquist, I.; Lundstrom, I.; Liedberg, B.; Parikh, A. N.; Allara D. L. *J. Phys. Chem.* **1997**, *106*, 33038.
(23) Lofgren, P.; Ahlstrom, P.; Chakarov, D. V.; Lausmaa, J.; Kasemo, B. *Surf. Sci.* **1996**, *367*, L13.
(24) Chakarov, D. V.; Osterlund, L.; Kasemo, B. *Vacuum* **1995**, *46*, 1109.
(25) Smith, R. S.; Huang, C.; Wong, E. K. L.; Kay, B. D. *Phys. Rev. Lett.* **1997**, *79* (5), 909.
(26) Lundgren, J. O. *J. Phys. Chem.* **1968**, *49*, 1068.
(27) Lundgren, J. O.; Olovsson, I. *Acta Crystallogr.* **1967**, *23*, 971.
(28) Delzeit, L.; Rowland, B.; Devlin, J. P. *J. Phys. Chem.* **1993**, *97*, 10312.
(29) Devlin, M. S. *Isr. J. Chem.* **1999**, *39*, 261.
(30) Clary, D. C.; Wang, L. C. *J. Chem. Soc., Faraday Trans.* **1997**, *93*, 2763.
(31) Gertner, B. J.; Hynes, J. T. *Science* **1996**, *271*, 1563.
(32) Novikov, V. *Grain Growth and Control of Microstructure and Texture in Polycrystalline Matirials*; CRC Press: New York, 1997.
(33) Delzeit, L.; Devlin, M. S.; Rowland, B.; Devlin J. P.; Buch, J. *J. Phys. Chem.* **1996**, *100*, 10076.
(34) Buch, V.; Delzeit, L.; Blackledge, C.; Devlin J. P *J. Phys. Chem.* **1996**, *100*, 3732.
(35) Barabasi, A. L.; Stanley, H. E. *Fractal Concepts in Surface Growth*; Cambridge University Press: Cambridge, 1995.
(36) Liu, Y.; Patterson, B. R. *Acta Metall. Mater.* **1993**, *41*, 2651.
(37) Lange, F. *J. Am. Ceram.* Soc. **1989**, *72*, 3.
(38) Stevenson, K. P.; Kimmel G. A.; Dohnalek, Z.; Smith R. S.; Kay B. D. *Science* **1999**, *283*, 1505.
(39) Brown, D. E.; George, S. M.; Huang, C.; Wong, E. K. L. Wong; Rider, K. B.; Smith, R. S.; Kay, B. D. *J. Phys. Chem.* **1996**, *100*, 4988.
(40) Haynes, D. R.; Tro, N. J.; George, S. M. *J. Phys. Chem.* **1992**, *96*, 8502.
(41) Blanchard J. L.; Roberts J. T. *Langmuir* **1994**, *10*, 3303.